Journal of Applied Physics

RESEARCH ARTICLE | DECEMBER 15 2023

Demonstration of high-throughput magnetic hysteresis measurements based on spintronic THz emission

M. F. DeCamp ; S. Bhatt ; M. T. Hossain ; W. Wu ; M. B. Jungfleisch

J. Appl. Phys. 134, 233901 (2023)
https://doi.org/10.1063/5.0165081

Journal of Applied Physics METHOD pubs.aip.org/aip/jap

Demonstration of high-throughput magnetic hysteresis measurements based on spintronic THz emission

Cite as: J. Appl. Phys. **134**, 233901 (2023); doi: 10.1063/5.0165081
Submitted: 26 June 2023 · Accepted: 18 November 2023 ·
Published Online: 15 December 2023

M. F. DeCamp,[a] S. Bhatt, M. T. Hossain, W. Wu, and M. B. Jungfleisch

AFFILIATIONS

Department of Physics and Astronomy, University of Delaware, Newark, Delaware 19716, USA

[a]**Author to whom correspondence should be addressed:** mdecamp@udel.edu

ABSTRACT

Spintronic terahertz (THz) emitters have been shown to be a cost-efficient source for use in time-domain THz spectroscopy. The use of external magnetic fields to control the polarity of the THz emission provides an opportunity to measure the magnetization of spintronic materials as well as shaping THz emission. Here, we demonstrate an efficient method of measuring magnetic hysteresis with material sensitivity and speed several orders of magnitude greater than typical magnetometry methods. In addition, we utilize the rapid control of material magnetization for lock-in detection in time-domain THz spectroscopy of spintronic emitters. The ability to rapidly control and measure the material magnetization on very small volumes provides an opportunity to study magnetic hetero-structures with sub-micron spatial resolution.

I. INTRODUCTION

The ultrafast manipulation of the electronic and atomic structure in solid state materials has long been used for the generation of pulsed terahertz (THz) radiation.[1,2] For example, upon sub-picosecond optical excitation, photo-conductive antennas can produce transient current which radiate fields with temporal components limited by carrier recombination and the optical excitation.[3,4] Recent advances in the sub-picosecond manipulation of material magnetization has given rise to ultrafast spintronic THz emitters,[5–10] a low cost alternative to other electronic charge based THz sources. Furthermore, spintronic THz emitters offer exciting opportunities to manipulate the radiation characteristics by controlling the design and structure of the material properties.[11–13]

Most spintronic THz emitters consist of a metallic multilayer thin film on an insulating substrate, whereby a ferromagnetic layer is deposited on a non-magnetic metal film (e.g., Pt or W).[8,14–16] When placed in a magnetic field with sufficient strength, the magnetization of the ferromagnetic material will be saturated. Upon sub-picosecond photo-excitation, rapid heating of the metallic film causes material demagnetization, resulting in a longitudinal spin current J_s that is proportional to the changing magnetization ($\frac{d\vec{M}}{dt} \propto J_s$). This longitudinal spin current is injected into the non-magnetic metallic layer, which is subsequently converted into a semi-uniform transient transverse electron current (J_c) by the inverse spin Hall effect.[5]

In the absence of an electrical potential gradient, Maxwell's equations dictate that in situations where J_c rapidly changes, electro-magnetic radiation will be generated. For spintronic emitters, in the dipole approximation, the radiating time-varying electric field is directly related to

$$\vec{E}(t) = K_1 \frac{d\vec{J_c}}{dt} = K_2 \frac{d^2\vec{M}}{dt^2}, \tag{1}$$

where K_1 and K_2 are proportionality constants related to the material properties and the geometry of the system. In addition, if the radiating field is measured at the focus of a collimated gaussian beam, additional modifications to the time-domain signal will be imposed due to filtering of the low-frequency radiation to geometric diffraction effects.[4,17,18] Provided that the photo-excitation is fast compared to magnetization recovery in the metallic film, the transient electron current will produce a time-varying electric field with temporal components dictated by the carrier dynamics.[8,9] Therefore, by directly measuring the radiating fields, one can indirectly measure the temporal dynamics associated with the sub-picosecond photo-excitation.

Previous studies investigated several aspects of magnetic- and electric-field control of spintronic THz emission. For example, Schneider *et al.* investigated the magnetic-field dependent THz emission in TbFe/Pt bi-layers and correlated the results with magnetometry.[19] On the other hand, Agarwal and co-workers recently demonstrated nonlinear electric-field control of spintronic THz emitters utilizing the magneto-electric effect in Pt/CoFeB hetero-structures fabricated on the top of the piezo-electric substrate.[20] Furthermore, Kong *et al.* showed that inhomogeneous magnetic fields can be used to tailor the THz polarization,[13] while Wu *et al.* utilized the magnetization texture in a meta-material made of a magnetic hetero-structure to control the THz polarization.[12] Very recently, Agarwal and colleagues proposed an approach to record the magnetic hysteresis loop by sweeping the THz pulse amplitude as a function of the magnetic field.[21,22] By doing so, they demonstrated a THz spintronic magnetometer capable of recording the hysteresis loop without contributions from the diamagnetic substrate. However, the optimal acquisition parameters for THz magnetometry and an enhanced signal-to-noise ratio of the hysteresis loops based on an ac modulation of the biasing magnetic field have not been demonstrated until now.

In this paper, we demonstrate time-domain THz spectroscopy (TDTS) for rapid measurement of magnetic hysteresis in spintronic THz emitters and correlate our results with standard vibrating sample magnetometry (VSM). This technique can measure the magnetic coercivity of the spintronic emitter in the fraction of the time of traditional magnetic methods using less than 0.1% of the necessary material, opening the possibility of imaging the distribution of sample magnetization with micrometer scale resolution.[23] In addition, as the ferromagnetic magnetization is easily saturated by a modulated magnetic field, we demonstrate that it is possible to magnetically modify the THz signal for lock-in detection for TDTS.

II. EXPERIMENTAL SETUP

In a typical TDTS measurement, an ultrafast THz pump field modifies the electro-optic response and/or photo-conductivity in a solid and a time-delayed ultrafast optical probe field measures the change in the optical properties of the material.[1,2,24,25] In circumstances where the frequency response of the detection medium is larger than constituent frequencies of the transient electric field, stroboscopic pump–probe measurements can directly measure the free-space electric field of the propagating THz field.

Our experimental setup is based upon a standard TDTS method using free-space electro-optic sampling[24,25] and is shown in Fig. 1. The laser is a titanium doped sapphire laser oscillator producing approximately 800 nm, 50 fs pulses at a repetition rate of 82 MHz with an average power of 200 mW. Upon entering the TDTS setup, the light was split using a thin optical beam splitter to both excite the spintronic device and perform free-space electro-optic sampling on the resulting emission. All experiments were performed at room temperature and ambient atmospheric conditions.

The optical pump beam was focused onto the emitter using a 150 mm lens, representing an optical spot size on the sample of less than 100 μm in diameter. The metallic layer of the emitter was placed in near direct contact with a silicon collimating lens (BATOP CSL-20) using a cellophane tape. The measured transverse acceptance of the Si lens was about 300 μm, suggesting that a large

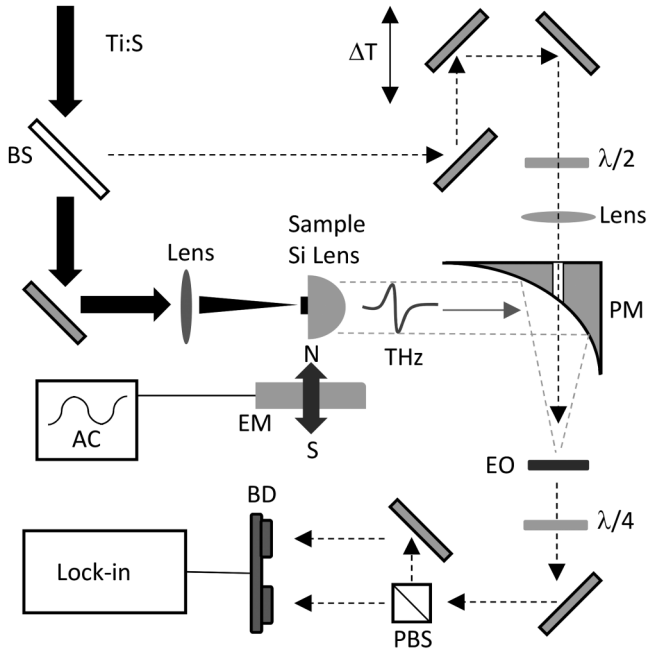

FIG. 1. Setup schematic of the TDTS setup. EM: electromagnet, BD: balanced detector, PBS: polarizing beamsplitter, PM: parabolic mirror, EO: 1 mm Thick ZnTe, BS: optical beamsplitter.

majority of the generated radiation was collected for TDTS. However, due to the index of refraction mismatch between the silicon lens and the surrounding air, only $\sim 50\%$ of the forward generated THz field was transmitted.

For free-space electro-optic sampling, the collimated THz radiation was focused onto the electro-optic (EO) crystal by a 200 mm off-axis parabolic metallic mirror. The optical probe beam was transmitted through a computer controlled time-delay line, a quarter-waveplate, and focused onto the EO crystal using a 250 mm lens. The resulting optical spot size of the optical probe beam at the EO crystal was less than the focused THz radiation. The polarization state of the optical probe beam was analyzed using a polarizing beam splitter (NEWPORT GLAN-Laser) and collected by a silicon-balanced detector (ThorLabs PDB210A), see Fig. 1. To assist in the temporal and spatial overlap of the THz field and optical probe beam, the spintronic emitter/silicon lens pair was replaced by a commercial photoconductive antenna (ThorLabs PCA-800), which produced peak free-space electro-optic signals almost 2 orders of magnitude larger than the spintronic THz emitter.

For lock-in detection, the emitted THz field was modulated by either chopping the optical pump-beam or by modifying the magnetic field created by an electromagnet, and the output of the balanced detector was measured by a Stanford Research Systems (SRS) lock-in amplifier. The electromagnet was a UXCELL 12 V lifting magnet, with a measured internal resistance 11.5 Ω, and an inner bore diameter of 30 mm. Measurement of the magnetic field at the surface of the electromagnet followed the oscillating voltage with peak fields of up to 75 G.

III. EXPERIMENTAL RESULTS

The studied spintronic emitter is a metallic tri-layer comprised of Ta(3 nm)/CoFeB(2 nm)/Pt(3 nm) deposited by sputtering deposition at room temperature on a double-side polished, $5 \times 5\,\mathrm{mm}^2$ sapphire substrate. For sample characterization, VSM measurements were taken at room temperature and at a sample rate of 1 data point per second. VSM measurements indicate that the ferromagnetic material has a coercivity of about 25 Oe and a saturation magnetization of about 200 emu/cm^3 [see Fig. 3(c)].

A typical TDTS measurement from the spintronic emitter using a 1 mm thick ZnTe (110) elctro-optic crystal is shown in Fig. 2. When the direction of the applied magnetic field is inverted, the TDTS responds in kind, a common characteristic of spintronic emitters. The peak optical phase rotation measured by the ZnTe was in excess of $\frac{\Delta\phi}{\phi} = 4 \times 10^{-6}$ resulting in a measured peak free-space electric field of ~70 V/m. Subsequent measurements using a 250 μm GaP (110) electro-optic crystal (see Fig. 2, inset) suggest that the peak field was at least four times greater. However, for the magnetic hysteresis experiments described here THz field measurements were made using the ZnTe given the significant improvement in signal to noise.

To determine if the electromagnet was sufficient to saturate the CoFeB magnetization, the time-delay of the TDTS system was placed at the peak of the electro-optic signal and the applied magnetic field was modulated using a digital function generator (SRS model DS-340). Due to geometric limitations associated with the silicon lens and the aluminum optical mount, the sample was placed about 15 mm from the surface of the electromagnet. Under these conditions, the function generator has sufficient power to drive the spintronic emitter to saturation at frequencies up to approximately 50 Hz.

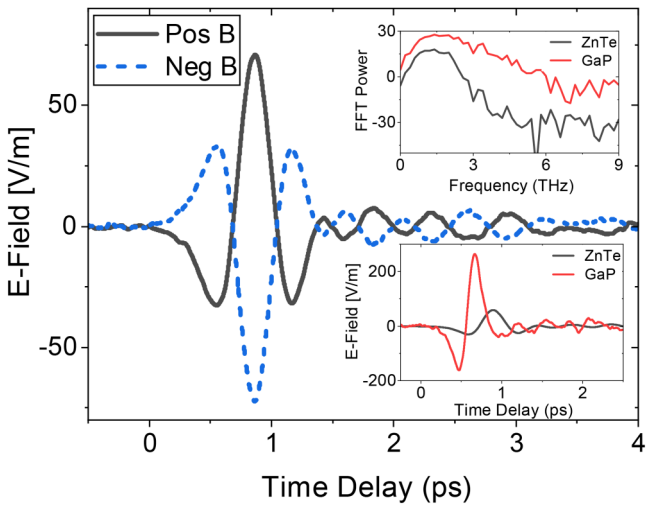

FIG. 2. Typical TDTS measurement of the spintronic emitter with different static applied magnetic fields. Inset top: FFT power spectrum of TDTS signal. Inset bottom: TDTS with GaP (red) and ZnTe (black) as detecting crystals.

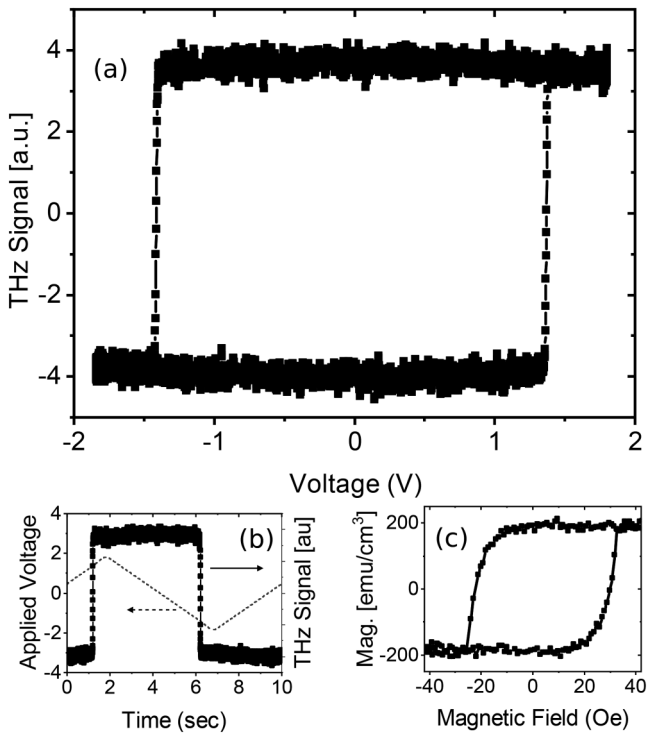

FIG. 3. (a) Magnetic hysteresis loop measured by TDTS with a modulated magnetic field operating at 0.1 Hz. (b) Peak THz signal and voltage applied to the electromagnet as a function of time. (c) Magnetic hysteresis of the sample as measured by VSM.

To accurately measure the magnetic hysteresis, temporal differences between the driving current and the lock-in amplifier were minimized by measuring the magnetic response to various pulse shapes. Two prototypical voltage shapes were used (square and triangle waves) and the lock-in amplifier was set with a time constant of 1 ms, which was faster than the recording rate of the data acquisition board (set at 500 Hz). Under these configurations, a full magnetic cycle was possible for each driving frequency chosen, representing hysteresis acquisition speeds of 1000 times faster than the single VSM measurement. Furthermore, as the detection region was governed by the focal geometry of the pump laser rather than the entire sample, the volume of the material that was measured was at least 3 orders of magnitude less than the VSM measurement, suggesting that hysteresis measurements are possible in very small sample volumes, potentially enabling spatially resolved magnetometry measurements at fast speeds.

For each magnetic hysteresis measurement, the time-delay of the TDTS was placed at its maximum signal. Depending on the driving frequency, between 6 and 200 magnetic cycles were averaged together to create the THz-magnetic hysteresis curve. Under these conditions, a total of about 1–10 min of data collection was used for each averaged hysteresis loop. When the square wave pulse train was applied (not shown), the magnetic pulse immediately

causes a flip in the sample magnetization such that the time delay between the voltage pulse and the lock-in signal could be calibrated. For the subsequent measurements, the voltage pulse was restricted to a triangle wave.

A typical THz response to the oscillating magnetic field of 0.1 Hz and an average of 20 voltage cycles is shown in Fig. 3(b). When the THz signal is plotted as a function of applied voltage [see Fig. 3(a)], a characteristic magnetic hysteresis curve is clearly visible. In this geometry, the electromagnet can drive the sample to saturation at an applied voltage of about 1.5 volts, with a switching time of less than 25 ms, consistent with the maximum switching rate that was possible with the digital function generator.

It should be noted that the relatively fast time constant on the lock-in amplifier was chosen to minimize temporal effects associated with the rapid measurement. In particular, hysteresis measurements taken with longer time constants and, thus, significantly higher signal-to-noise, displayed qualitatively the same behavior in a single magnetic cycle. However, as the lock-in time constant became comparable, or exceeded, 25 ms, the data acquisition methodology significantly influenced the signal response.

Qualitative similarities are apparent between the magnetic THz hysteresis and that measured by the VSM [Fig. 3(c)]. However, the change of THz polarity as a function of the applied magnetic field is significantly more rapid than the VSM measurement. In contrast to the direct measurement of material magnetization in VSM, TDTS of spintronic devices measures the time-derivative of the material magnetization [see Eq. (1)], likely resulting in the observed differences in the magnetic hysteresis. These results suggest that using THz emission to measure magnetic hysteresis response in spintronic emitters could be more sensitive than traditional magnetometer measurements.

As the frequency of the voltage being applied to the electromagnet was raised, the observed switching field monotonically increased (see Fig. 4), consistent with prior results.[26,27] At the lowest frequency measured (0.01 Hz), the observed transition voltage results in a magnetic field at the surface of the electromagnet of about 50 G, consistent with measured coercivity, given the spatial separation between the sample and the electromagnet. At frequencies above ∼ 5 Hz, the combination of the observed 25 ms switching time, current limits on the electromagnet, and the power limitations of the function generator made the THz driven coercivity measurements increasingly unreliable. However, we expect that these limitations can be reduced by an improved design and engineering of the electromagnet. While current experiments are being designed to study this frequency dependence more closely, this observation clearly demonstrates the sensitivity of using TDTS for measuring magnetic hysteresis.

As demonstrated by the THz magnetic hysteresis, the ability to drive material magnetization at higher frequencies provides an attractive method for lock-in detection. In this case, for field modifications greater than 50 Hz, the function generator could not provide sufficient power to drive the electromagnet necessitating the need for an additional analog audio amplifier. With the audio amplifier, frequencies up to 1 kHz were possible with the existing electromagnet.

As a proof-of-concept demonstration, TDTS measurements using both traditional optical chopping methods and *magnetic chopping* methods are shown in Fig. 5. Each of the TDTS curves was an average of 30 independent scans with a time-constant of 100 ms on the lock-in amplifier, representing about 3 s of averaging at each time delay point. Optical chopping at 10 kHz represented a noise floor of $\frac{\Delta\phi}{\phi} \sim 10^{-8}$. Measurements using optical chopping at 750 Hz demonstrate a significant increase in the noise floor ($\frac{\Delta\phi}{\phi} \sim 5 \times 10^{-7}$), likely due to inductive pickup in the balanced photodiode.

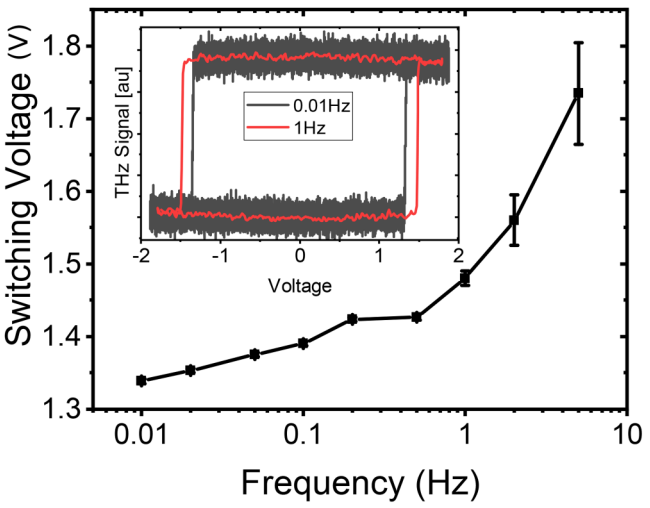

FIG. 4. Coercivity voltage as a function of electromagnet frequency. Inset: THz-magnetic hysteresis loop measured by TDTS at 0.01 (black) and 1 Hz (red).

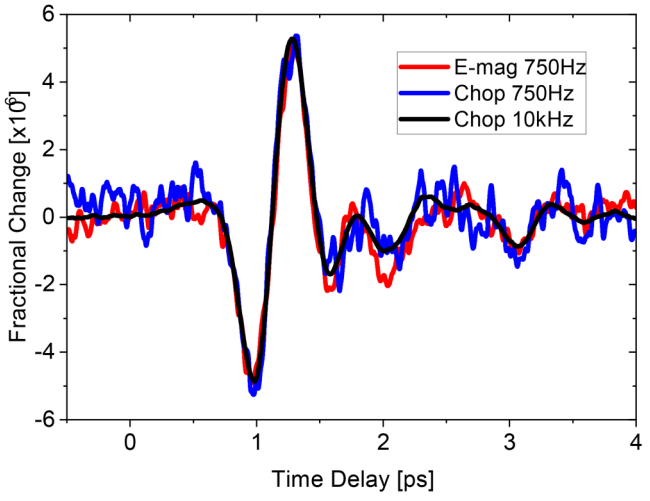

FIG. 5. TDTS of the spintronic emitter using optical chopping at 750 Hz (blue) and 10 kHz (black) and magnetic switching at 750 Hz (red).

Subsequent measurements with the electromagnet show similar results. In particular, the noise floor is half that of the optical chopping ($\frac{\Delta\phi}{\phi} \sim 2.5 \times 10^{-7}$) due to the fact that magnetic modulation results in a signal that is doubled. This is a consequence of the polarity of the spintronic THz emission inverting upon changing the direction of the magnetization by 180° (see Fig. 2). With further improvements to the electromagnet and audio amplifier configuration, chopping at higher rates, and thus higher signal-to-noise ratios, should be possible.

IV. CONCLUSION

In conclusion, using TDTS spectroscopy methods, we have demonstrated a technique to quickly measure magnetic hysteresis curves in spintronic THz emitters, paving the way for high-throughput wireless magnetic hysteresis measurements. Given the high fidelity of the hysteresis, and minimal material requirements, these results suggest that this technique could be expanded to perform micron scale spatially resolved coercivity measurements. In addition, we have demonstrated a proof-of-concept magnetic chopper based on the magnetic hysteresis, providing a method to isolate the magnetic response from other external stimuli.

SUPPLEMENTARY MATERIAL

In an effort to quantify the inhomogeneity of the magnetic field supplied by the electro-magnet at the sample, a three-dimensional, numerical simulation using the electromagnetic PDEsolver is supplied in MATLAB. The results of which are shown in the supplementary material.

ACKNOWLEDGMENTS

M.F.D. would like to thank Anna Stein for technical assistance. M.B.J. acknowledges support by NSF through the University of Delaware Materials Research Science and Engineering Center, Grant No. DMR-2011824.

AUTHOR DECLARATIONS

Conflict of Interest

The authors have no conflicts to disclose.

Author Contributions

M. F. DeCamp: Conceptualization (lead); Data curation (lead); Formal analysis (lead); Funding acquisition (equal); Investigation (lead); Methodology (lead); Project administration (lead); Resources (lead); Software (lead); Supervision (lead); Validation (lead); Visualization (lead); Writing – original draft (lead); Writing – review & editing (equal). **S. Bhatt:** Resources (supporting); Writing – review & editing (supporting). **M. T. Hossain:** Data curation (supporting); Writing – review & editing (supporting). **W. Wu:** Resources (supporting); Writing – review & editing (supporting). **M. B. Jungfleisch:** Formal analysis (supporting); Funding acquisition (equal); Writing – original draft (supporting); Writing – review & editing (equal).

DATA AVAILABILITY

The data that support the findings of this study are available from the corresponding author upon reasonable request.

REFERENCES

[1]M. Beard, G. Turner, and C. Schumettenmaer, "Terahertz spectroscopy," J. Phys. Chem. B **106**, 7146 (2002).
[2]C. Schumuttenmaer, "Exploring dynamics in the far-infrared with terahertz spectroscopy," Chem. Rev. **104**, 1759 (2004).
[3]D. You, R. R. Jones, P. H. Bucksbaum, and D. R. Dykaar, "Generation of high-power sub-single-cycle 500 fs electromagnetic pulse," Opt. Lett. **18**, 290 (1993).
[4]E. Budiarto, N. Pu, S. Jeong, and J. Bokor, "Near-field propagation of terahertz pulses from a large-aperture antenna," Opt. Lett. **23**, 213 (1998).
[5]T. Kampfrath, M. Battiato, P. Maldonado, G. Eilers, J. Nötzold, S. Mährlein, V. Zbarsky, F. Freimuth, Y. Mokrousov, S. Blügel, M. Wolf, I. Radu, P. M. Oppeneer, and M. Münzenberg, "Terahertz spin current pulses controlled by magnetic heterostructures," Nat. Nanotechnol. **8**, 256–260 (2013).
[6]T. Seifert, S. Jaiswal, U. Martens, J. Hannegan, L. Braun, P. Maldonado, F. Freimuth, A. Kronenberg, J. Henrizi, I. Radu, E. Beaurepaire, Y. Mokrousov, P. M. Oppeneer, M. Jourdan, G. Jakob, D. Turchinovich, L. M. Hayden, M. Wolf, M. Muenzenberg, M. Klaeui, and T. Kampfrath, "Efficient metallic spintronic emitters of ultrabroadband terahertz radiation," Nat. Photonics **10**, 483–488 (2016).
[7]J. Walowski and M. Muenzenberg, "Perspective: Ultrafast magnetism and THz spintronics," J. Appl. Phys. **120**, 140901 (2016).
[8]W. Wu, C. Yaw Ameyaw, M. F. Doty, and M. B. Jungfleisch, "Principles of spintronic THz emitters," J. Appl. Phys. **130**, 091101 (2021).
[9]M. Wang, Y. Zhang, L. Guo, M. Lv, P. Wang, and X. Wang, "Spintronics based terahertz sources," Crystals **12**, 1661 (2022).
[10]E. T. Papaioannou and R. Beigang, "THz spintronic emitters: A review on achievements and future challenges," Nanophotonics **10**, 1243–1257 (2021).
[11]W. Wu, S. Lendinez, M. Taghipour Kaffash, R. D. Schaller, H. Wen, and M. B. Jungfleisch, "Modification of terahertz emission spectrum using microfabricated spintronic emitters," J. Appl. Phys. **128**, 103902 (2020).
[12]W. Wu, S. Lendinez, M. T. Kaffash, R. D. Schaller, H. Wen, and M. B. Jungfleisch, "Controlling polarization of spintronic THz emitter by remanent magnetization texture," Appl. Phys. Lett. **121**, 052401 (2022).
[13]D. Kong, X. Wu, B. Wang, T. Nie, M. Xiao, C. Pandey, Y. Gao, L. Wen, W. Zhao, C. Ruan, J. Miao, Y. Li, and L. Wang, "Broadband spintronic terahertz emitter with magnetic-field manipulated polarizations," Adv. Opt. Mater. **7**, 1900487 (2019).
[14]T. Seifert, S. Jaiswal, M. Sajadi, G. Jakob, S. Winnerl, M. Wolf, M. Klaeui, and T. Kampfrath, "Ultrabroadband single-cycle terahertz pulses with peak fields of 300 kV cm^{-1} from a metallic spintronic emitter," Appl. Phys. Lett. **110**, 252402 (2017).
[15]R. Schneider, M. Fix, R. Heming, S. M. de Vasconcellos, M. Albrecht, and R. Bratschitsch, "Magnetic-field-dependent THz emission of spintronic TbFe/Pt layers," ACS Photonics **5**, 3936–3942 (2018).
[16]D. Yang, J. Liang, C. Zhou, L. Sun, R. Zheng, S. Luo, Y. Wu, and J. Qi, "Powerful and tunable THz emitters based on the Fe/Pt magnetic heterostructure," Adv. Opt. Mater. **4**, 1944–1949 (2016).
[17]P. Kuzel, M. Khazan, and J. Kroupa, "Spatiotemporal transformations of ultrashort terahertz pulses," J. Opt. Soc. Am. B **16**, 1795 (1999).
[18]A. Gurtler, C. Winnewisser, H. Helm, and P. Jepsen, "Terahertz pulse propagation in the near field and the far field," J. Opt. Soc. Am. A **17**, 74 (2000).
[19]R. Schneider, M. Fix, R. Heming, S. Michaelis de Vasconcellos, M. Albrecht, and R. Bratschitsch, "Magnetic-field-dependent THz emission of spintronic TbFe/Pt layers," ACS Photonics **5**, 3936–3942 (2018).
[20]P. Agarwal, L. Huang, S. Ter Lim, and R. Singh, "Electric-field control of nonlinear THz spintronic emitters," Nat. Commun. **13**, 4072 (2022).

[21]P. Agarwal, Y. Yang, J. Laurembaum, R. Medwal, M. Battiato, and R. Singh, "Terahertz spintronic magnetometer (TSM)," Appl. Phys. Lett. **120**, 161104 (2022).
[22]P. Agarwal, R. Medwal, A. Kumar, H. Asada, Y. Fukuma, R. S. Rawat, M. Battiato, and R. Singh, "Ultrafast photo-thermal switching of terahertz spin currents," Adv. Funct. Mater. **31**, 2010453 (2021).
[23]F. Stiewe, T. Winkel, T. Kleinke, T. Tubandt, H. Heyen, L. Vollroth, U. Martens, C. Mueller, J. McCord, J. Walowski, and M. Muenzenberg, "Magnetic domain scanning imaging using phase-sensitive THz-pulse detection," AIP Adv. **12**, 095010 (2022).
[24]Q. Wu and X. Zhang, "Free-space electrooptic sampling of terahertz beams," Appl. Phys. Lett. **67**, 3523–3525 (1995).
[25]A. Nahata, A. Weling, and T. Heinz, "A wideband coherent terahertz spectroscopy system using opticalrectification and electro-optic sampling," Appl. Phys. Lett. **69**, 2321 (1996).
[26]G. Vertesy and A. Magni, "Frequency dependence of coercive properties," J. Magn. Magn. Mater. **265**, 7 (2003).
[27]R. Groessinger, N. Mehboob, M. Kriegisch, A. Bachmaier, and P. Pippan, "Frequency dependence of the coercivity of soft magnetic materials," IEEE Trans. Magn. **48**, 1473 (2012).